Estimation of Both Junction Temperature and Load Current of IGBTs from Output Voltage of Gate Driver

Hiromu Yamasaki, Katsuhiro Hata and Makoto Takamiya
The University of Tokyo, Tokyo, Japan

***Abstract*—For the online condition monitoring of IGBTs, a new estimation method of both the junction temperature (T_J) and the load current (I_L) of IGBTs using a momentary high-Z gate driving (MHZGD) from the output voltage (V_{OUT}) of the gate driver is proposed, which can be integrated into the gate driver ICs. T_J is estimated from V_{OUT} difference during and after the MHZGD period, and I_L is estimated from V_{OUT} during MHZGD. In the 110 switching measurements at 11 different T_J's from 25 °C to 125 °C and 10 different I_L's from 12.5 A to 80 A for each of the three IGBTs, T_J and I_L estimation errors in a low test cost parameter determination method are + 4.9 °C / − 8.4 °C and + 1.1 A / − 4.3 A, respectively. In contrast, T_J and I_L estimation errors in a parameter determination method with small error are + 4.9 °C / − 8.1 °C and + 1.0 A / − 1.8 A, respectively.**

I. Introduction

In order to achieve reliable power electronics systems, online condition monitoring for power devices is required to predict power device failures. The development goals of the online condition monitoring in this paper include: (1) estimation of both the junction temperature (T_J) and the load current (I_L) without using temperature sensors and current sensors, because T_J and I_L are important parameters that determine the reliability of power devices; and (2) measurement from the gate terminal of a power device that can be integrated into gate driver ICs. Many papers have been published on the estimation of T_J and/or I_L [1-16], however, there have been no papers achieving the two development goals. In [7], only I_L is estimated using a momentary high-Z gate driving (MHZGD) and it is necessary to give T_J as a known value for I_L estimation. To solve the problems, in this paper, a new estimation method of both T_J and I_L of IGBTs using MHZGD from the output voltage (V_{OUT}) of the gate driver is proposed.

II. Measurement of ΔV and $V_{OUT,MHZ}$ Using MHZGD

A. *Momentary High-Z Gate Driving (MHZGD) to Estimate T_J and I_L*

Fig. 1 shows a circuit schematic of a gate driver and an IGBT. The target of this work is to estimate both T_J and I_L from V_{OUT}. Fig. 2 shows waveforms of a conventional gate driving and MHZGD [7] at turn-off of IGBT. In the conventional gate driving shown in Fig. 2 (a), V_{OUT} at the

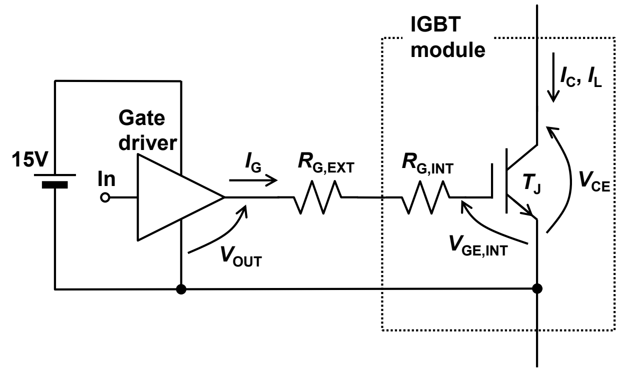

Fig. 1. Circuit schematic of gate driver and IGBT.

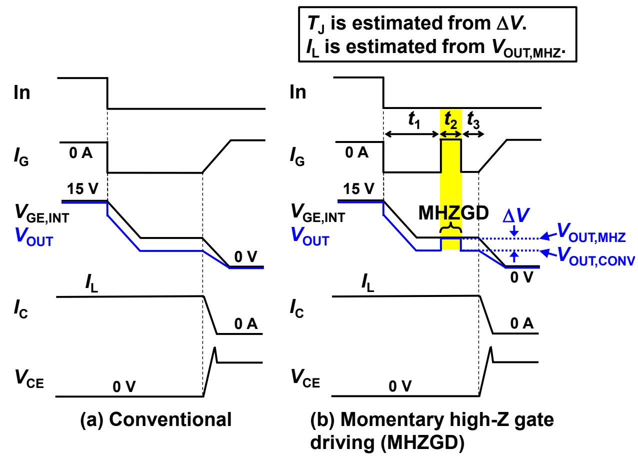

Fig. 2. Waveforms at turn-off. (a) Conventional gate driving. (b) MHZGD[7].

Miller plateau is not equal to the internal gate-emitter voltage ($V_{GE,INT}$) due to I_G ($R_{G,INT} + R_{G,EXT}$) drop, where I_G is the gate driving current, $R_{G,INT}$ is the internal gate resistance of IGBT, and $R_{G,EXT}$ is the external gate resistance. In MHZGD [7] shown in Fig. 2 (b), the period from the start of turn-off to the end of the Miller plateau is divided into three parts and defined as t_1, t_2, and t_3. t_2 and t_3 must be during the Miller plateau period. In MHZGD, I_G is zero during t_2. In this work, the zero I_G is achieved using the digital gate driver (DGD) [17]. During t_2, V_{OUT} is equal to $V_{GE,INT}$ because of zero I_G, and this V_{OUT} is defined as $V_{OUT,MHZ}$. V_{OUT} during t_3 is defined as $V_{OUT,CONV}$, and the difference between $V_{OUT,MHZ}$ and $V_{OUT,CONV}$ is defined as ΔV, where $\Delta V = |I_G|$ ($R_{G,INT} + R_{G,EXT}$). Assuming that I_G is constant in this paper because of the constant current-source based DGD [17], ΔV is linearly dependent on T_J, because $R_{G,INT}$ is linearly dependent on T_J [1]. Therefore, in this paper, T_J is estimated from ΔV, while I_L is estimated from $V_{OUT,MHZ}$. The principle of estimating I_L from $V_{OUT,MHZ}$ is the same as [7], while T_J is not estimated and must be known in advance in [7].

B. Measurement Setup

Fig. 3 shows the photo of the measurement setup of the double pulse test of IGBT module (2MBI100VA-060-50, 600 V, 100 A) at 300V for the estimation of T_J and I_L. The DGD IC [17] drives the low side of the IGBT module. T_J is assumed to be equal to the hot plate temperature. $R_{G,EXT}$ is zero. In this paper, after the switching measurements are performed under 110 different conditions with 11 different T_J's from 25 °C to 125 °C in 10 °C steps and 10 different I_L's from 12.5 A to 80 A in 7.5 A steps for each of the three IGBTs and V_{OUT} waveform data are saved, the estimations of T_J and I_L from ΔV and $V_{OUT,MHZ}$ are done. V_{OUT} waveforms are measured using the differential probe and ΔV and $V_{OUT,MHZ}$ are extracted from the V_{OUT} waveforms. In the future, the measurement of ΔV and $V_{OUT,MHZ}$ can be done with an A/D converter, which can be integrated on DGD IC

C. Measurement of ΔV and $V_{OUT,MHZ}$

Fig. 4 shows the measured waveforms at T_J = 25 °C and I_L = 80 A during the turn-off of IGBT. In this paper, t_2 is fixed to 2 μs. ΔV and $V_{OUT,MHZ}$ generated by MHZGD are clearly observed. Please note that MHZGD has no effect

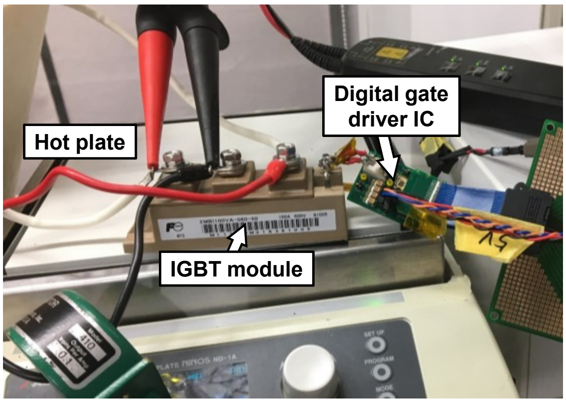

Fig. 3. Measurement setup of double pulse test.

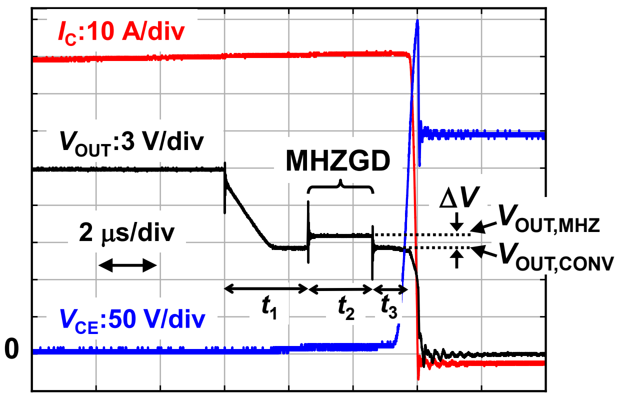

Fig. 4. Measured waveforms at T_J = 25 °C and I_L = 80 A during turn-off.

on the switching loss and V_{CE} overshoot. Fig. 5 shows the measured V_{OUT} waveforms of T_J = 25 °C and 125 °C at I_L = 12.5 A. With increasing T_J, $V_{OUT,MHZ}$ is reduced, because the threshold voltage of IGBT is reduced. Fig. 6 shows the measured V_{OUT} waveforms of I_L = 12.5 A to 80 A at T_J = 25 °C. $V_{OUT,MHZ}$ increases with increasing I_L. Fig. 7 shows the overall view of measured $V_{OUT,CONV}$ and $V_{OUT,MHZ}$ under 60 different conditions with 6 different T_J's ranging from 25 °C to 125 °C and 10 different I_L's ranging from 12.5 A to 80 A. ΔV is the difference between $V_{OUT,MHZ}$ and $V_{OUT,CONV}$. In the next chapter, the methods for estimating T_J and I_L from ΔV and $V_{OUT,MHZ}$, respectively, will be explained.

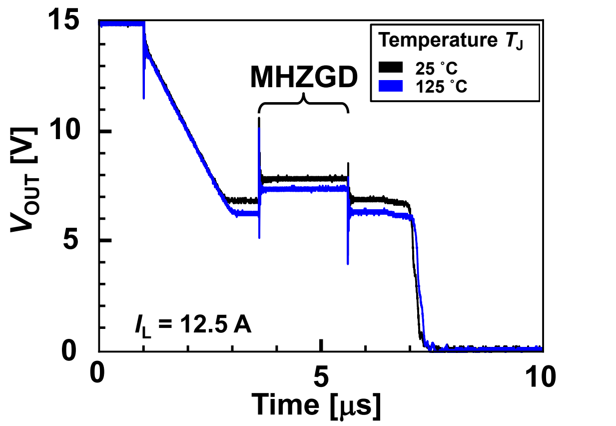

Fig. 5. Measured V_{OUT} waveforms of T_J = 25 °C and 125 °C at I_L = 12.5 A.

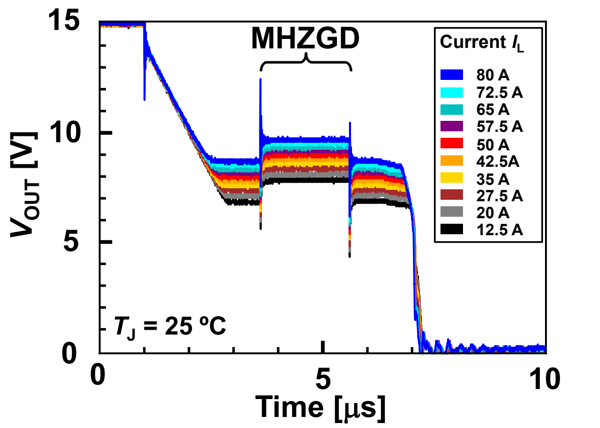

Fig. 6. Measured V_{OUT} waveforms of I_L = 12.5 A to 80 A at T_J = 25 °C.

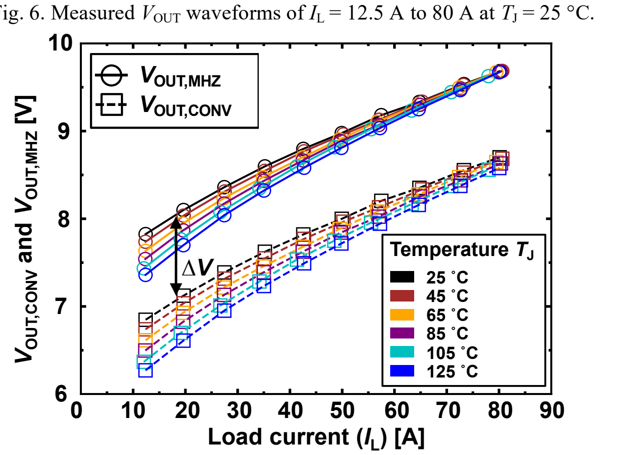

Fig. 7. Measured $V_{OUT,CONV}$ and $V_{OUT,MHZ}$ under 60 different conditions with 6 different T_J's and 10 different I_L's.

III. T_J AND I_L ESTIMATIONS FROM ΔV AND $V_{OUT,MHZ}$

A. Overview of Proposed T_J and I_L Estimation

Fig. 8 shows an overview of the proposed T_J and I_L estimation from ΔV and $V_{OUT,MHZ}$. When the measured ΔV and $V_{OUT,MHZ}$ are given, T_J is estimated using Eq. (1) and I_L is estimated using Eqs. (2) to (4), where $k(T_J)$ is the T_J-dependent constant, $V_{TH}(T_J)$ is the T_J-dependent threshold voltage of IGBT, T_R is the room temperature (25 °C) whose unit is absolute temperature, $k(T_R)$ is $k(T_J)$ at $T_J = T_R$, $V_{TH}(T_R)$ is $V_{TH}(T_J)$ at $T_J = T_R$, and a, b, α, β, and γ are constants. Comparing [7] with this paper, Eqs. (2) to (4) are identical to [7], and only Eq. (1) is newly added in this paper. The values of seven parameters (a, b, α, β, γ, $k(T_R)$, and $V_{TH}(T_R)$) are determined by the calibration measurements.

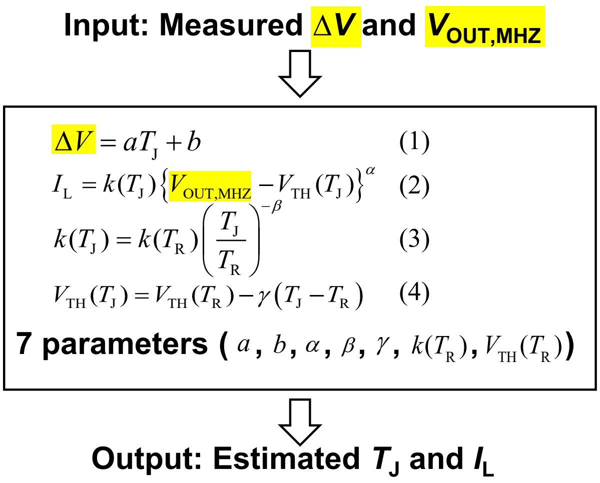

Fig. 8. Overview of proposed T_J and I_L estimation from ΔV and $V_{OUT,MHZ}$.

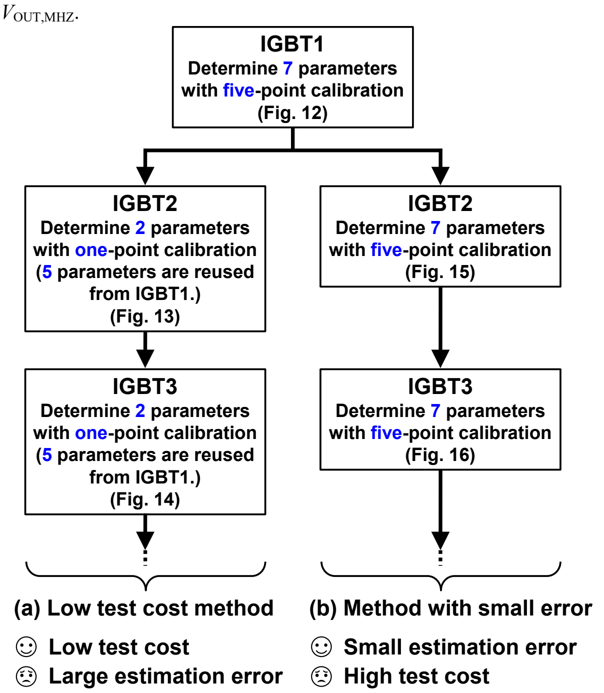

Fig. 9. Two parameter determination methods compared in this paper. (a) Low test cost method. (b) Method with small error.

B. Parameter Determination Methods for T_J and I_L Estimation

Fig. 9 shows two parameter determination methods for multiple IGBTs compared in this paper. Fig. 9 (a) shows a low test cost method, where a five-point calibration is performed for the first IGBT (IGBT1), and a one-point calibration is performed for the second and subsequent IGBTs (IGBT2 and IGBT3). The details of the five-point and the one-point calibrations will be explained later. Fig. 9 (b) shows a method with small error, where a five-point calibration is performed for all IGBTs. The two methods have a trade-off in terms of the estimation error and the test cost for the calibrations. The low test cost method has the disadvantage of large estimation error, while the method with small error has the disadvantage of high test cost.

Fig. 10 (a) shows the steps for the five-point calibration to find the values of seven parameters shown in Fig. 8. In Step 1, V_{OUT} waveforms under five conditions at (T_J, I_L) = (25 °C, 12.5 A), (25 °C, 42.5 A), (25 °C, 80 A), (125 °C, 12.5 A), and (125 °C, 80 A) are measured. In Step 2, two ΔV's are extracted from V_{OUT} waveforms at (T_J, I_L) = (25 °C, 12.5 A) and (125 °C, 12.5 A). In Step 3, a and b in Eq. (1) are determined by the curve fitting as shown in Fig. 11 (a). In Step 4, three $V_{OUT,MHZ}$'s are extracted from V_{OUT} waveforms at (T_J, I_L) = (25 °C, 12.5 A), (25 °C, 42.5 A), and (25 °C, 80 A). In Step 5, $k(T_R)$, $V_{TH}(T_R)$, and α in Eqs. (2) to (4) are determined by the curve fitting as shown in Fig. 11 (b). In Step 6, two $V_{OUT,MHZ}$'s are extracted from V_{OUT} waveforms at (T_J, I_L) = (125 °C, 12.5 A) and (125 °C, 80 A). In Step 7, $k(T_J = 125$ °C) and $V_{TH}(T_J = 125$ °C) in Eqs. (3) to (4) are determined by the curve fitting as shown in Fig. 11 (c). In Step 8, β and γ are determined by Eqs. (3) and (4) as shown in Figs. 11 (d) and (e), respectively, which completes the five-point calibration.

Fig. 10 (b) shows the steps for the one-point calibration to find the values of two parameters (b and $V_{TH}(T_R)$). In the one-point calibration, five parameters (a, α, β, γ, and $k(T_R)$) of IGBT1 are reused to other IGBTs to reduce the test cost. The intention of the one-point calibration is to express the

Step 1	Measure V_{OUT} waveforms under 5 conditions: (T_J, I_L) = (25˚C, 12.5 A), (25˚C, 42.5 A), (25˚C, 80 A), (125˚C, 12.5 A), (125˚C, 80 A)
Step 2	Extract ΔV's from V_{OUT} waveforms at (25˚C, 12.5 A), (125˚C, 12.5 A)
Step 3	Derive a and b by curve fitting (Fig. 11(a))
Step 4	Extract $V_{OUT,MHZ}$'s V_{OUT} waveforms at (25˚C, 12.5 A), (25˚C, 42.5 A), (25˚C, 80 A)
Step 5	Derive $k(T_R)$, $V_{TH}(T_R)$, and α (Fig. 11(b))
Step 6	Extract $V_{OUT,MHZ}$'s from V_{OUT} waveforms at (125˚C, 12.5 A), (125˚C, 80 A)
Step 7	Derive $k(T_J$=125˚C) and $V_{TH}(T_J$=125˚C) (Fig. 11(c))
Step 8	Derive β and γ (Fig. 11(d)(e))

(a)

Step 1	Measure V_{OUT} waveform at (T_J, I_L) = (25˚C, 12.5 A)
Step 2	Extract $V_{OUT,MHZ}$ and ΔV from V_{OUT} waveform
Step 3	Derive b and $V_{TH}(T_R)$ by curve fitting

(b)

Fig. 10. Steps for calibrations. (a) Five-point calibration. (b) One-point calibration.

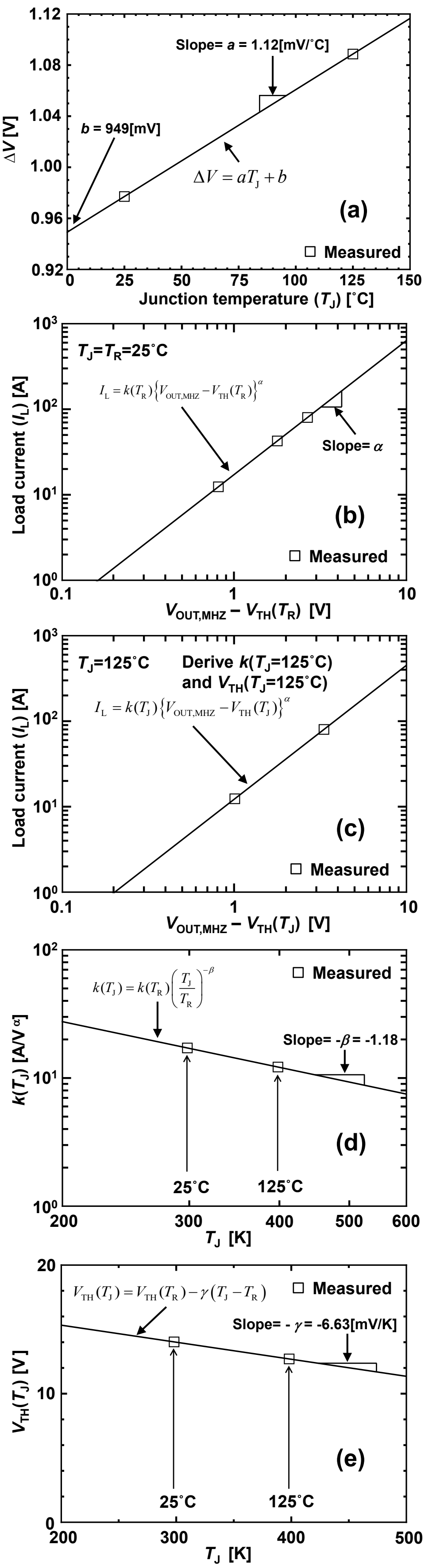

Fig. 11. Example of parameter determination in IGBT1. (a) Step 3 in Fig. 10 (a). (b) Step 5 in Fig. 10 (a). (c) Step 7 in Fig. 10 (a). (d) and (e) Step 8 in Fig. 10 (a).

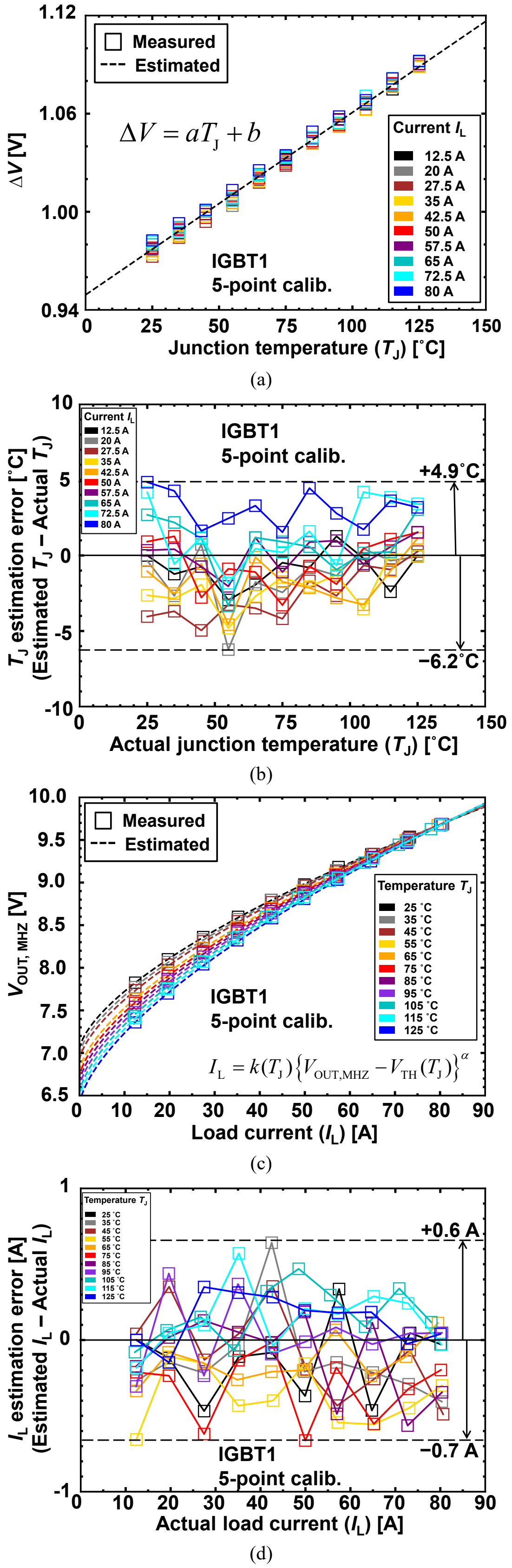

Fig. 12. Results of IGBT1 using five-point calibration, which is same for both methods. (a) Measured and estimated T_J dependence of ΔV at 10 different I_L's. (b) T_J estimation error. (c) Measured and estimated I_L dependence of $V_{OUT,MHZ}$ at 11 different T_J's. (d) I_L estimation error.

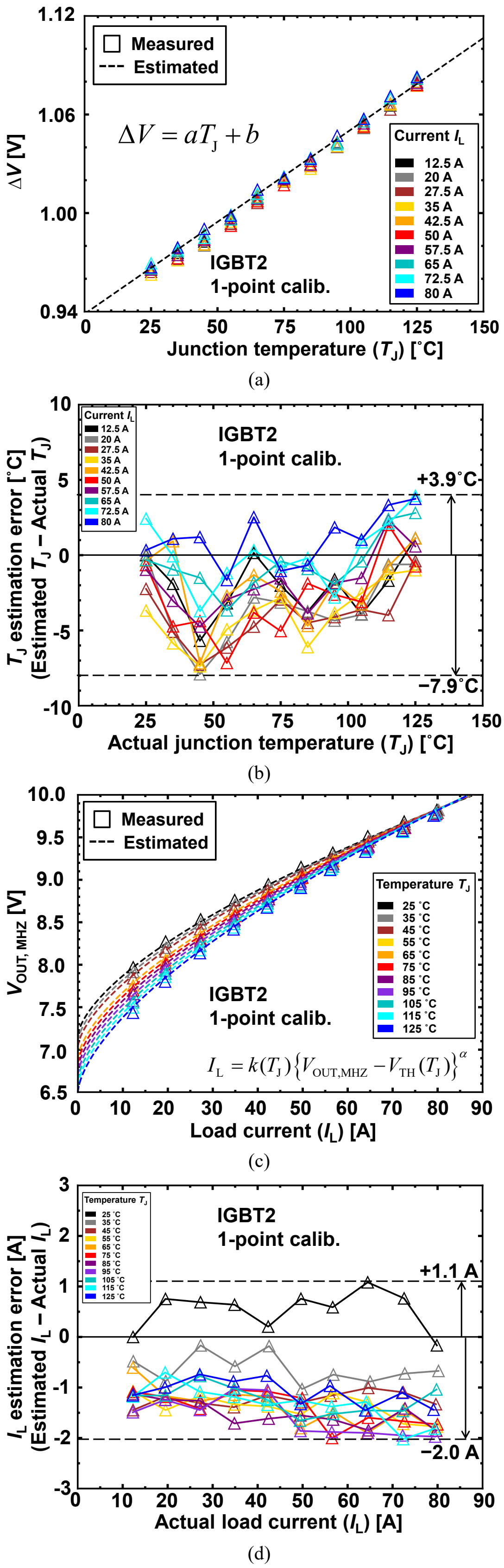

Fig. 13. Results of IGBT2 using one-point calibration in low test cost method. (a) Measured and estimated T_J dependence of ΔV at 10 different I_L's. (b) T_J estimation error. (c) Measured and estimated I_L dependence of $V_{OUT,MHZ}$ at 11 different T_J's. (d) I_L estimation error.

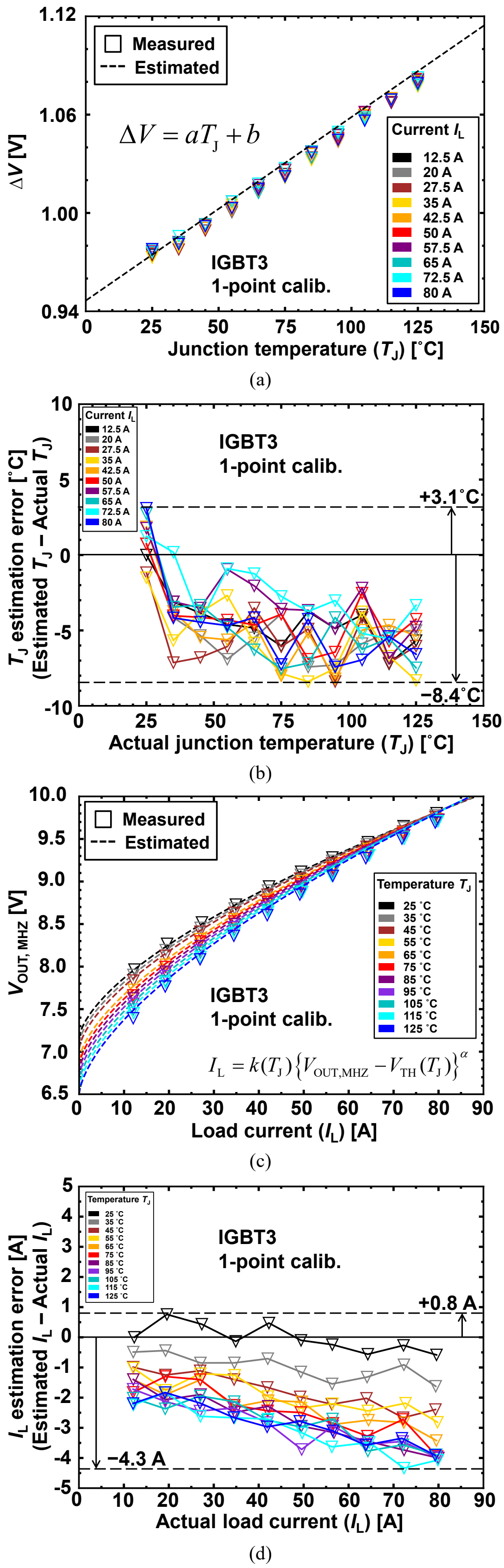

Fig. 14. Results of IGBT3 using one-point calibration in low test cost method. (a) Measured and estimated T_J dependence of ΔV at 10 different I_L's. (b) T_J estimation error. (c) Measured and estimated I_L dependence of $V_{OUT,MHZ}$ at 11 different T_J's. (d) I_L estimation error.

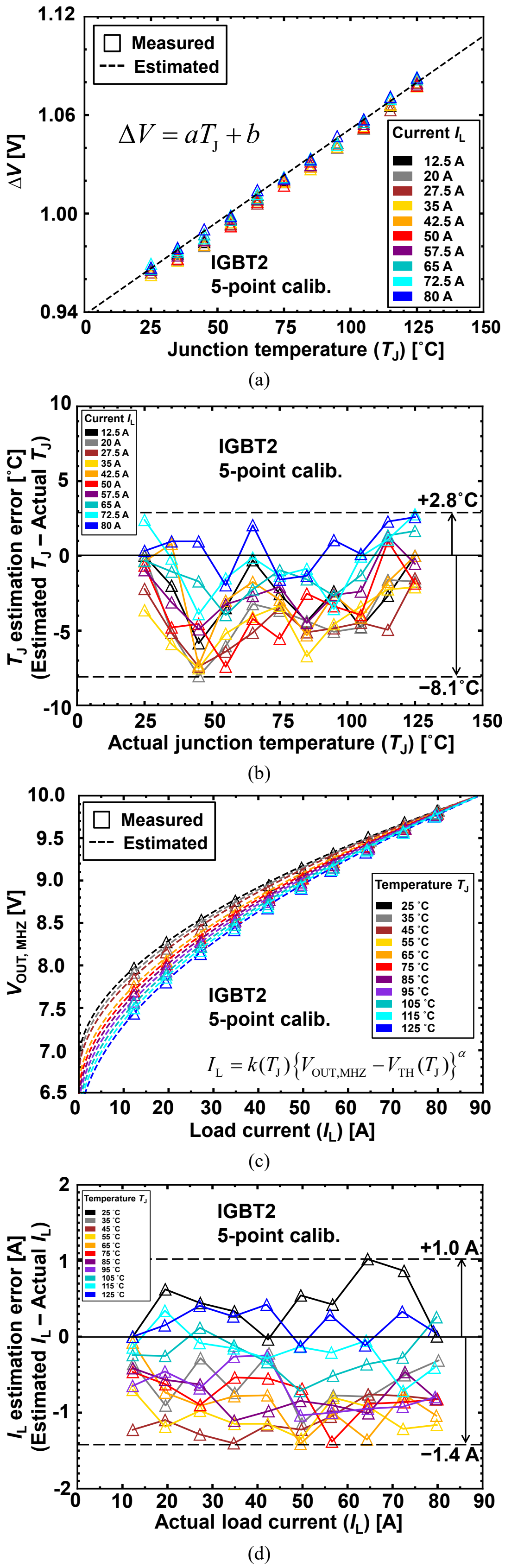

Fig. 15. Results of IGBT2 using five-point calibration in method with small error. (a) Measured and estimated T_J dependence of ΔV at 10 different I_L's. (b) T_J estimation error. (c) Measured and estimated I_L dependence of $V_{OUT,MHZ}$ at 11 different T_J's. (d) I_L estimation error.

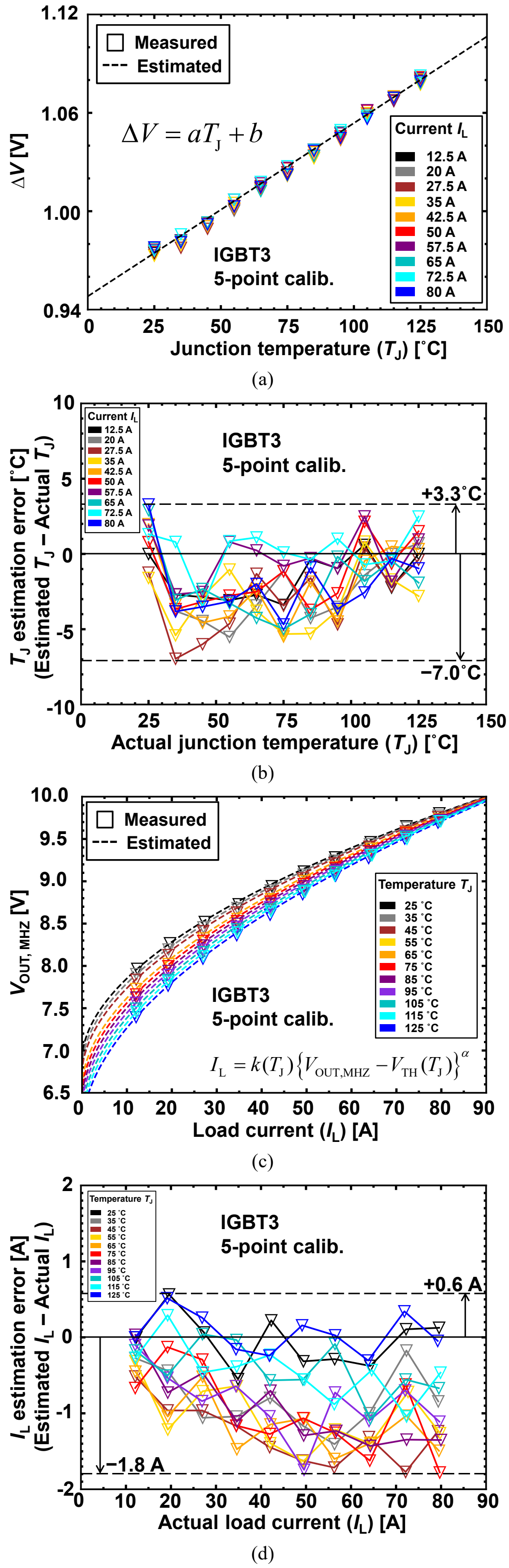

Fig. 16. Results of IGBT3 using five-point calibration in method with small error. (a) Measured and estimated T_J dependence of ΔV at 10 different I_L's. (b) T_J estimation error. (c) Measured and estimated I_L dependence of $V_{OUT,MHZ}$ at 11 different T_J's. (d) I_L estimation error.

Table I Measured conditions and calibrated parameters for three IGBTs. (a) Low test cost method. (b) Method with small error.

Measured conditions (T_J, I_L)	Sample	Calibrated parameters	Parameters						
			a [mV/°C]	b [mV]	$V_{TH}(T_R)$ [V]	$k(T_R)$ [A/V$^{\alpha}$]	α	β	γ [mV/K]
(25°C, 12.5A), (25°C, 42.5A), (25°C, 80A), (125°C, 12.5A), (125°C, 80A)	IGBT1	a, b, $V_{TH}(T_R)$, $k(T_R)$, α, β, γ	1.12	949	7.01	17.2	1.57	1.18	6.63
(25°C, 12.5A)	IGBT2	b, $V_{TH}(T_R)$		938	7.16				
	IGBT3	b, $V_{TH}(T_R)$		947	7.16				

(a)

Measured conditions (T_J, I_L)	Sample	Calibrated parameters	Parameters						
			a [mV/°C]	b [mV]	$V_{TH}(T_R)$ [V]	$k(T_R)$ [A/V$^{\alpha}$]	α	β	γ [mV/K]
(25°C, 12.5A), (25°C, 42.5A), (25°C, 80A), (125°C, 12.5A), (125°C, 80A)	IGBT1	a, b, $V_{TH}(T_R)$, $k(T_R)$, α, β, γ	1.12	949	7.01	17.2	1.57	1.18	6.63
	IGBT2	a, b, $V_{TH}(T_R)$, $k(T_R)$, α, β, γ	1.13	938	7.12	15.9	1.62	1.30	7.57
	IGBT3	a, b, $V_{TH}(T_R)$, $k(T_R)$, α, β, γ	1.06	948	7.08	14.9	1.67	1.27	7.78

(b)

Table II Summaries of T_J and I_L estimation errors. (a) Low test cost method. (b) Method with small error.

Sample	Calibration method	T_J estimation error [°C]			I_L estimation error [A]		
		Max	Min	Max-Min	Max	Min	Max-Min
IGBT1	5-point	+4.9	-6.2	11.1	+0.6	-0.7	1.3
IGBT2	1-point	+3.9	-7.9	11.8	+1.1	-2.0	3.1
IGBT3	1-point	+3.1	-8.4	11.5	+0.8	-4.3	5.1
IGBT1-IGBT3		+4.9	-8.4	13.3	+1.1	-4.3	5.4

(a)

Sample	Calibration method	T_J estimation error [°C]			I_L estimation error [A]		
		Max	Min	Max-Min	Max	Min	Max-Min
IGBT1	5-point	+4.9	-6.2	11.1	+0.6	-0.7	1.3
IGBT2	5-point	+2.8	-8.1	10.9	+1.0	-1.4	2.4
IGBT3	5-point	+3.3	-7.0	10.3	+0.6	-1.8	2.4
IGBT1-IGBT3		+4.9	-8.1	13.0	+1.0	-1.8	2.8

(b)

variation of each IGBT in terms of b and $V_{TH}(T_R)$. In Step 1, a V_{OUT} waveform at (T_J, I_L) = (25 °C, 12.5 A) is measured. In Step 2, b and $V_{TH}(T_R)$ in Eqs. (1) and (4) are determined by the curve fitting.

Tables I (a) and (b) show the measured conditions and the calibrated parameters obtained by the low test cost method (Fig. 9 (a)) and the method with small error (Fig. 9 (b)), respectively, for three IGBTs (IGBT1 to IGBT3). In the low test cost method (Table I (a)), the five parameters (a, α, β, γ, and $k(T_R)$) of IGBT1 are reused to IGBT2 and IGBT3 to reduce the test cost.

C. T_J and I_L Estimation Results

As shown in Fig. 9, Figs. 12 to 16 show T_J and I_L estimation results in IGBT1 to IGBT3. Figs. 12 to 14 show T_J and I_L estimation results using the low test cost method, while Figs. 12, 15, and 16 show T_J and I_L estimation results using the method with small error. Fig. 12 shows the results of IGBT1 using the five-point calibration, which is the same for both methods. Fig. 13 shows the results of IGBT2 using the one-point calibration in the low test cost method. Fig. 14 shows the results of IGBT3 using the one-point calibration in the low test cost method. Fig. 15 shows the results of IGBT2 using the five-point calibration in the method with small error. Fig. 16 shows the results of IGBT3 using the five-point calibration in the method with small error.

The details of Figs. 12 to 16 are explained using Fig. 12 as a representative example. Fig. 12 (a) shows the measured and estimated T_J dependence of ΔV at 10 different I_L's. The estimated curve is calculated using Eq. (1) and Table I (a). ΔV increases with increasing T_J because of increasing $R_{G,INT}$. ΔV's are in the range of 0.96 V to 1.10 V, which is reasonably explained by $|I_G|$ $R_{G,INT}$ = 108 mA × 9 Ω = 0.972 V. Fig. 12 (b) shows the T_J estimation error in Fig. 12 (a). Please note that T_J estimation errors at (T_J, I_L) = (25 °C, 12.5 A) and (125 °C, 12.5 A) are 0 °C, because the calibration of a and b is done at (T_J, I_L) = (25 °C, 12.5 A) and (125 °C, 12.5 A). T_J estimation error in the range of 25 °C to 125 °C and I_L =

12.5 A to 80 A is within + 4.9 °C / − 6.2 °C. Fig. 12 (c) shows the measured and estimated I_L dependence of $V_{OUT,MHZ}$ at 11 different T_J's. The estimated curves are calculated using Eqs. (2) to (4) and Table I (a). Fig. 12 (d) shows the I_L estimation error in Fig. 12 (c). I_L estimation error in the range of 12.5 A to 80 A and T_J = 25 °C to 125 °C is within + 0.6 A / − 0.7 A.

Tables II (a) and (b) show summaries of T_J and I_L estimation errors in the low test cost method (Fig. 9 (a)) and the method with small error (Fig. 9 (b)), respectively, for IGBT1 to IGBT3. Comparing the estimation errors using the two methods, the T_J and I_L estimation errors (+ 4.9 °C / − 8.4 °C and + 1.1 A / − 4.3 A) of the low test cost method is larger those (+ 4.9 °C / − 8.1 °C and + 1.0 A / − 1.8 A) of the method with small error, as expected. The method with small error, however, requires five measurements at T_J = 25 °C and 125 °C for each IGBT as shown in Step 1 in Fig. 10 (a), which is not practical, because the test cost is too high. Therefore, in conclusion, the low test cost method is recommended in this paper.

D. Comparison with Previous Works

Table III shows a comparison table of T_J and/or I_L estimation for the condition monitoring. This paper is the first work to successfully estimate both T_J and I_L from the measured values obtained from the gate terminal.

Table III Comparison table of T_J and/or I_L estimation.

Reference	[1]	[2]	[5]	[6]	[7]	This work
Estimated value	T_J	T_J	I_L	T_J, I_L	I_L	T_J, I_L
Measured value	Peak of I_G	$V_{GE,EXT}$	I_G	$V_{EE'}$	V_{OUT}	V_{OUT}
Measured value from gate terminal	Yes	Yes	Yes	No	Yes	Yes
T_J range [°C]	20 – 140*	10 – 100*	25 – 75	25 – 105*	25 – 125	25 – 125
I_L range [A]	50 – 1200*	15 – 325*	1 – 50	100 – 550*	5 – 80	12.5 – 80
Max estimation error	N.A.	7.5 °C	0.5 A	N.A.	7.7 %	8.4 °C, 4.3 A(1) 8.1 °C, 1.8 A(2)
Additional circuits	Peak hold	None	Plateau detector	Peak hold, integrator	Switch	Constant current DGD

*Obtained from graph, (1) Low test cost method, (2) Method with small error

IV. Conclusions

For the online condition monitoring of IGBTs, this paper is the first work to successfully estimate both T_J and I_L using MHZGD from V_{OUT}. T_J is estimated from ΔV, while I_L is estimated from $V_{OUT,MHZ}$. In the 110 switching measurements at 11 different T_J's from 25 °C to 125 °C and 10 different I_L's from 12.5 A to 80 A for each of the three IGBTs, T_J and I_L estimation errors in the low test cost method are + 4.9 °C / − 8.4 °C and + 1.1 A / − 4.3 A, respectively. In contrast, T_J and I_L estimation errors in the method with small error are + 4.9 °C / − 8.1 °C and + 1.0 A / − 1.8 A, respectively. In this paper, the low test cost method is recommended, because the test cost of the method with small error is too high.

Acknowledgment

This work was partly supported by JST-Mirai Program, Grant Number JPMJMI20E1, Japan.

References

[1] N. Baker, S. Munk-Nielsen, F. Iannuzzo, and M. Liserre, "IGBT junction temperature measurement via peak gate current," *IEEE Trans. on Power Electronics*, vol. 31, no. 5, pp. 3784-3793, May 2016.

[2] C. H. van der Broeck, A. Gospodinov, and R. W. De Doncker, "IGBT junction temperature estimation via gate voltage plateau sensing," *IEEE Trans. on Industry Applications*, vol. 54, no. 5, pp. 4752-4763, Sep-Oct. 2018.

[3] J. Liu, G. Zhang, Q. Chen, L. Qi, Z. Qin, J. Wang, and Y. Geng, "Online junction temperature extraction and aging detection of IGBT via miller plateau width," in *Proc. IEEE Appl. Power Electron, Conf. Expo.*, Mar. 2018, pp. 2813-2820.

[4] J. Brandelero, J. Ewanchuk, and S. Mollov, "On-line virtual junction temperature measurement via DC gate current injection," in *Proc. 10th International Conference on Integrated Power Electronics Systems*, Mar. 2018, pp. 1-7.

[5] J. Chen, W. J. Zhang, A. Shorten, J. Yu, M. Sasaki, T. Kawashima, H. Nishio, and W. T. Ng, "A smart IGBT gate driver IC with temperature compensated collector current sensing," *IEEE Trans. on Power Electronics*, vol. 34, no. 5, pp. 4613-4627, May 2019.

[6] V. K. Sundaramoorthy, E. Bianda, R. Bloch, and F. Zurfluh, "Simultaneous online estimation of junction temperature and current of IGBTs using emitter-auxiliary emitter parasitic inductance," in *Proc. International Exhibition and Conference for Power Electronics, Intelligent Motion, Renewable Energy and Energy Management*, May 2014, pp. 1-8.

[7] H. Yamasaki, R. Katada, K. Hata, and M. Takamiya, "Momentary high-Z gate driving (MHZGD) at miller plateau for IGBT load current estimation from gate driver," in *Proc. IEEE Energy Conversion Congress and Exposition - Asia*, May 2021, pp. 1698-1704.

[8] U. Choi, F. Blaabjerg, S. Jorgensen, S. Munk-Nielsen, and B. Rannestad, "Reliability improvement of power converters by means of condition monitoring of IGBT modules," *IEEE Trans. on Power Electronics*, vol. 32, no. 10, pp. 7990-7997, Oct. 2017.

[9] Y. Avenas, L. Dupont, and Z. Khatir, "Temperature measurement of power semiconductor devices by thermo-sensitive electrical parameters—a review," *IEEE Trans. on Power Electronics*, vol. 27, no. 6, pp. 3081-3092, Jun. 2012.

[10] B. Ji, X. Song, W. Cao, V. Pickert, Y. Hu, J. W. Mackersie, and G. Pierce, "In situ diagnostics and prognostics of solder fatigue in IGBT modules for electric vehicle drives," *IEEE Trans. on Power Electronics*, vol. 30, no. 3, pp. 1535-1543, Mar. 2015.

[11] N. Baker, L. Dupont, S. Munk-Nielsen, F. Iannuzzo, and M. Liserre, ''IR camera validation of IGBT junction temperature measurement via peak gate current,'' *IEEE Trans. on Power Electronics*, vol. 32, no. 4, pp. 3099-3111, Apr. 2017.

[12] R. Mandeya, C. Chen, V. Pickert, and R. T. Naayagi, ''Prethreshold voltage as a low-component count temperature sensitive electrical parameter without self-heating,'' *IEEE Trans. on Power Electronics*, vol. 33, no. 4, pp. 2787-2791, Apr. 2018.

[13] N. Baker, and F. Iannuzzo, ''The temperature dependence of the flatband voltage in high-power IGBTs,'' *IEEE Trans. on Industry Applications*, vol. 66, no. 7, pp. 5581-5584, Jul. 2019.

[14] F. Wuest, S. Trampert, S. Janzen, S. Straube, and M. S. Ramelow, ''Comparison of temperature sensitive electrical parameter based methods for junction temperature determination during accelerated aging of power electronics,'' *Microelectron. Reliability*, vol. 88-90, pp. 534-539, Sep. 2018.

[15] H. Luo, Y. Chen, P. Sun, W. Li, and X. He, ''Junction temperature extraction approach with turn-off delay time for high-voltage high-power IGBT modules,'' *IEEE Trans. on Power Electronics*, vol. 31, no. 7, pp. 5122-5132, Jul. 2016.

[16] Y. Chen, H. Luo, W. Li, X. He, F. Iannuzzo, and F. Blaabjerg, ''Analytical and experimental investigation on a dynamic thermo-sensitive electrical parameter with maximum dIC/dt during turn-off for high power trench gate/field-stop IGBT modules,'' *IEEE Trans. on Power Electronics*, vol. 32, no. 8, pp. 6394-6404, Aug. 2017.

[17] K. Miyazaki, S. Abe, M. Tsukuda, I. Omura, K. Wada, M. Takamiya, and T. Sakurai, "General-purpose clocked gate driver IC with programmable 63-level drivability to optimize overshoot and energy loss in switching by a simulated annealing algorithm," *IEEE Trans. on Industry Applications*, vol. 53, no. 3, pp. 2350-2357, May-Jun. 2017.